arXiv:1509.08436v1 [hep-ph] 28 Sep 2015

A covariant model for the negative parity resonances of the nucleon

G. Ramalho

International Institute of Physics, Federal University of Rio Grande do Norte, Av. Odilon Gomes de Lima 1722, Capim Macio, Natal-RN 59078-400, Brazil

E-mail: gilberto.ramalho2013@gmail.com

Abstract. We present a model for the $\gamma^* N \to N^*$ helicity amplitudes, where N is the nucleon and N^* is a negative parity nucleon excitation, member of the $SU(6)$-multiplet $[70, 1^-]$. The model combines the results from the single quark transition model for the helicity amplitudes with the results of the covariant spectator quark model for the $\gamma^* N \to N^*(1535)$ and $\gamma^* N \to N^*(1520)$ transitions. With the knowledge of the amplitudes $A_{1/2}$ and $A_{3/2}$ for those transitions we calculate three independent coefficients defined by the single quark transition model and make predictions for the helicity amplitudes associated with the $\gamma^* N \to N^*(1650)$, $\gamma^* N \to N^*(1700)$, $\gamma^* N \to \Delta(1620)$, and $\gamma^* N \to \Delta(1700)$ transitions. In order to facilitate the comparison with future experimental data at high Q^2, we provide also simple parametrizations for the amplitudes, compatible with the expected falloff at high Q^2.

1. Introduction

One of the challenges in the modern physics is the description of the internal structure of the baryons and mesons. The electromagnetic structure of the nucleon N and the nucleon resonances N^* can be accessed through the $\gamma^* N \to N^*$ reactions, which depend of the (photon) momentum transfer squared Q^2 [1, 2, 3, 4]. The data associated with those transitions are represented in terms of helicity amplitudes and have been collected in the recent years at Jefferson Lab, with increasing Q^2 [1]. The new data demands the development of theoretical models based on the underlying structure of quarks and quark-antiquark states (mesons) [1, 2]. Those models may be used to guide future experiments as the ones planned for the Jlab–12 GeV upgrade, particularly for resonances in the second and third resonance region [energy $W = 1.4$–1.8 GeV] (see figure 1) [1]. In that region there are several resonances N^* from the multiplet $[70, 1^-]$ of $SU(6) \otimes O(3)$, characterized by a negative parity [2, 5, 6]. According with the single quark transition model (SQTM), when the electromagnetic interaction is the result of the photon coupling with just one quark, the helicity amplitudes of the $[70, 1^-]$ members depend only on three independent functions of Q^2: A, B and C [6, 7]. In this work we use the covariant spectator quark model [1, 7, 8] developed for the $\gamma^* N \to N^*(1520)$ and $\gamma^* N \to N^*(1535)$ transitions, also members of $[70, 1^-]$, to calculate those functions [9, 10]. Since the covariant spectator quark model breaks the $SU(2)$-flavor symmetry, we restrict our study to reactions with proton targets (average on the SQTM coefficients) [7]. Later on, with the knowledge of the functions A, B, and C we predict the helicity amplitudes for transitions associated with the remaining members of the multiplet $[70, 1^-]$ [7].

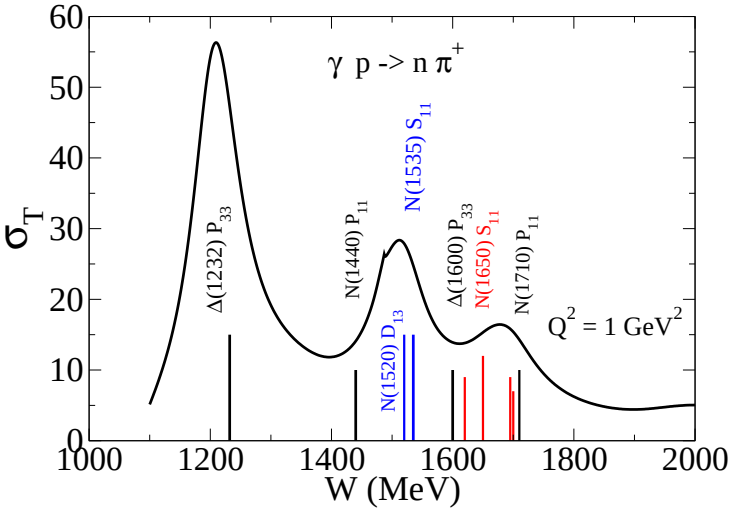

Figure 1. Representation of the $\gamma p \to n\pi^+$ cross section. The graph define the 3 resonance regions. The vertical lines represent resonant states described by the covariant spectator quark model. At red we indicate the states studded in this work. At blue are the states used as input.

2. Covariant Spectator Quark Model

The covariant spectator quark model is based on the formalism of the covariant spectator theory [11]. In the covariant spectator quark model, baryons are treated as three-quark systems. The baryon wave functions are derived from the quark states according with the $SU(6) \otimes O(3)$ symmetry group. A quark is off-mass-shell, and free to interact with the photon fields, and other two quarks are on-mass-shell [8, 12, 13, 14]. Integrating over the quark-pair degrees of freedom we reduce the baryon to a quark-diquark system, where the diquark can be represented as an on-mass-shell spectator particle with an effective mass m_D [8, 9, 10, 12, 14].

The electromagnetic interaction with the baryons is described by the photon coupling with the constituent quarks in the relativistic impulse approximation. The quark electromagnetic structure is represented in terms of the quark form factors parametrized by a vector meson dominance mechanism [8, 14, 15]. The parametrization of the quark current was calibrated in the studies of the nucleon form factors data [8], by the lattice QCD data for the decuplet baryon [14], and encodes effectively the gluon and quark-antiquark substructure of the constituent quarks. The quark current has the general form [8, 14]

$$j_q^\mu(Q^2) = j_1(Q^2)\gamma^\mu + j_2(Q^2)\frac{i\sigma^{\mu\nu}q_\nu}{2M}, \tag{1}$$

where M is the nucleon mass and j_i $(i = 1, 2)$ are the Dirac and Pauli quark form factors. In the $SU(2)$-flavor sector the functions j_i can also be decomposed into the isoscalar (f_{i+}) and the isovector (f_{i-}) components: $j_i = \frac{1}{6}f_{i+} + \frac{1}{2}f_{i-}\tau_3$, where τ_3 acts on the isospin states of baryons (nucleon or resonance). The details can be found in [8, 13, 14].

When the nucleon wave function (Ψ_N) and the resonance wave function (Ψ_R) are both expressed in terms of the single quark and quark-pair states, the transition current in impulse approximation as can be written [8, 12, 14]

$$J^\mu = 3\sum_\Gamma \int_k \bar{\Psi}_R(P_+, k) j_q^\mu \Psi_N(P_-, k), \tag{2}$$

where P_-, P_+, and k are the nucleon, the resonance, and the diquark momenta respectively. In the previous equation the index Γ labels the possible states of the intermediate diquark polarizations, the factor 3 takes account of the contributions from the other quark pairs by the symmetry, and the integration symbol represents the covariant integration over the diquark

on-mass-shell momentum. In the study of inelastic reactions we replace $\gamma^\mu \to \gamma^\mu - \frac{\not{q} q^\mu}{q^2}$ in equation (1). This procedure ensures the conservation of the transition current and it is equivalent to the use of the Landau prescription [7, 9, 10].

Using equation (2), we can express the transition current in terms of the quark electromagnetic form factor $f_{i\pm}$ $(i = 1, 2)$ and the radial wave functions ψ_N and ψ_R [8, 9, 10]. The radial wave functions are scalar functions that depend on the baryon (P) and diquark (k) momenta and parametrize the momentum distributions of the quark-diquark systems. From the transition current we can extract the form factors and the helicity transition amplitudes, defined in the rest frame of the resonance (final state), for the reaction under study [1, 2, 9, 10].

There are however some processes such as the meson exchanged between the different quarks inside the baryon, which cannot be reduced to simple diagrams with quark dressing. Those processes are regarded as arising from a meson exchanged between the different quarks inside the baryon and can be classified as meson cloud corrections to the hadronic reactions [10, 13, 16].

The covariant spectator quark model was used already in the study of several nucleon excitations including isospin 1/2 systems $N(1410), N(1520), N(1535), N(1710)$ [9, 10, 17] and the isospin 3/2 systems [18, 19, 20]. The model generalized to the $SU(3)$-flavor sector was also used to study the octet and decuplet baryons as well as transitions between baryons with strange quarks [16, 21]. In figure 1 the position of the nucleon excitations are represented and compared with the bumps of the cross sections. Based on the parametrization of the quark current (1) in term of the vector meson dominance mechanism, the model was extended to the lattice QCD regime (heavy pions and no meson cloud) [15, 18], to the nuclear medium [13] and to the timelike regime [22]. The model was also used to study the nucleon deep inelastic scattering [8, 23] and the axial structure of the octet baryon [24].

3. Results for $N(1535)$ and $N(1520)$

For the study of the states $N(1535)$ $(\frac{1}{2}^-)$ and $N(1520)$ $(\frac{3}{2}^-)$ it is necessary to specify the shape of the radial wave function of the nucleon and resonant states. The radial wave function can be represented using the dimensionless variable $\chi = \frac{(P-k)^2-(M_B-m_D)^2}{M_B m_D}$, where M_B is the mass of the baryon B. We choose in particular

$$\psi_N(P,k) = \frac{N_0}{m_D(\beta_2+\chi)(\beta_1+\chi)}, \qquad \psi_R(P,k) = \frac{N_1}{m_D(\beta_2+\chi)}\left[\frac{1}{\beta_1+\chi} - \frac{\lambda_R}{\beta_j+\chi}\right], \tag{3}$$

where N_0, N_1 are normalization constants, β_1, β_2 and β_j are momentum range parameters in units $M_B m_D$. We use $\beta_j = \beta_3$ for $N(1535)$ and $\beta_j = \beta_4$ for $N(1520)$. Those parameters are fixed by a fit to the the large Q^2 data [7, 10]. The coefficient λ_R is determined by an orthogonality condition between the nucleon and the state R. In the following we will use also the spectroscopic notation to represent the states $N(1535)$ (or $S11$) and $N(1535)$ (or $D13$). In addition we use M_S and M_D to represent the $S11$ and $D13$ masses, respectively.

3.1. State $N(1535)$

From the study of [7, 9] we conclude that we can write the amplitude $A_{1/2}$ for the $N(1535)$ state in terms of the Dirac transition form factor (F_1^*). The final result is then

$$A_{1/2} = -\frac{\sqrt{2}}{3} F_S \left(f_{1+} + 2 f_{1-}\tau_3\right) \mathcal{I}_{S11} \cos\theta_S, \qquad \mathcal{I}_{S11}(Q^2) = \int_k \frac{k_z}{|\mathbf{k}|} \psi_{S11}(P_+,k)\psi_N(P_-,k), \tag{4}$$

where $F_S = 2e\sqrt{\frac{(M_S+M)^2+Q^2}{8M(M_S^2-M^2)}}$ and $\mathcal{I}_{S11}$ is a covariant integral calculated on the $S11$ rest frame.

The result (4) is valid for large Q^2 since only valence quark effects are considered and it is the consequence of the observation that the Pauli transition form factor (F_2^*) vanishes for $Q^2 \gtrsim 1.5$

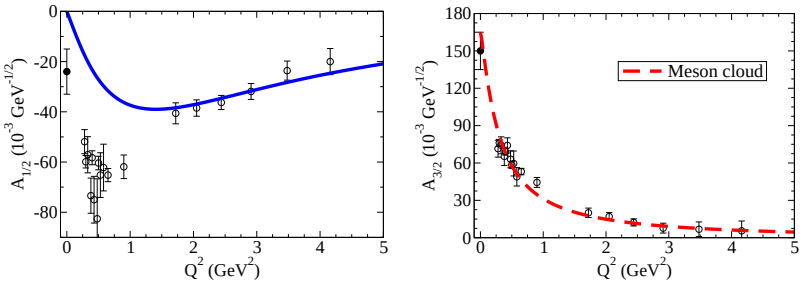

Figure 2. Results for the resonance $N(1520)$. The amplitude $A_{3/2}$ the result of meson cloud effects. was no contributions from valence quarks. Data from CLAS [3].

GeV^2, which is interpreted as the consequence of the cancellation between valence quark and meson cloud effects [9]. In this work we updated the model from [9] using the radial wave function ψ_R given by equation (3), in order to ensure the exact orthogonality between nucleon and $N(1535)$ states. In the process we introduce a new parameter (β_3) that is adjusted by the large Q^2 data (no meson cloud) [7].

3.2. State $N(1520)$

The model for from [10] can be used to calculate the electromagnetic transition form factors for the $\gamma^* N \to N(1520)$ transition, including the magnetic dipole G_M and the electric quadrupole G_E form factors, based in the effects of the valence quarks. One obtain then $G_E = -G_M$, where

$$G_M = \mathcal{R}(f_{1+} + 2f_{1-}\tau_3)\mathcal{I}_{D13} + \frac{M_D + M}{2M}(f_{2+} + 2f_{2-}\tau_3)\mathcal{I}_{D13}. \tag{5}$$

In the equations $\mathcal{R} = \frac{1}{3\sqrt{3}}\frac{M}{M_D - M}\sqrt{\frac{(M_D-M)^2+Q^2}{(M_D+M)^2+Q^2}}$, and $\mathcal{I}_{D13}(Q^2) = \int_k \frac{k_z}{|\mathbf{k}|}\psi_{D13}(P_+, k)\psi_N(P_-, k)$ is the new invariant integral defined at the resonance rest frame.

The result $G_M + G_E = 0$ is interesting, since it is consistent with the expected QCD behavior for large Q^2, but it is inconsistent with the data at low Q^2, that shows a significant magnitude for the amplitude $A_{3/2} \propto (G_M + G_E)$, near $Q^2 = 0$ [2, 7, 10]. In general, quark models predict small contributions for $A_{3/2}$ (20–40%) [7, 10]. There are however indications that the effects of the meson cloud contribution dominate the amplitude, as supported by the calculation from EBAC at Jefferson Lab [25]. Based on that information we represent the helicity amplitudes as

$$A_{1/2} = F_D\, G_M + \frac{1}{4} F_D\, G_4^\pi, \qquad A_{3/2} = \frac{\sqrt{3}}{4} F_D\, G_4^\pi, \tag{6}$$

where $F_D = \frac{e}{M}\sqrt{\frac{M_D - M}{M_D + M}}\sqrt{\frac{(M_D+M)^2+Q^2}{2M}}$. In the equations (6), G_4^π is a function that is not determined by the covariant spectator quark model (that predicts $G_4^\pi \equiv 0$) and parametrize the amplitude $A_{3/2}$ assuming the dominance of the pion/meson cloud effects. The function G_4^π is fitted to the data with a model inspired on the pion and meson cloud contributions for the $\gamma^* N \to \Delta$ transition [7, 10, 22]. The results from the amplitudes $A_{1/2}$ (valence quark) and $A_{3/2}$ (meson cloud) are presented on figure 2.

4. Single Quark Transition Model

The combination of the wave functions of a baryon (three-quark system) given by $SU(6) \otimes O(3)$ group and the description of electromagnetic interaction in impulse approximation leads to the so-called single quark transition model [6, 26]. In this context *single* means that only one quark couples with the photon. In these conditions the SQTM can be used to parametrize the transition current between two multiplets, in an operational form that includes only four independent terms, with coefficients exclusively dependent of Q^2.

State	Amplitude	
$N(1535)$	$A_{1/2}$	$\frac{1}{6}(A+B-C)\cos\theta_S$
$N(1520)$	$A_{1/2}$	$\frac{1}{6\sqrt{2}}(A-2B-C)\cos\theta_D$
	$A_{3/2}$	$\frac{1}{2\sqrt{6}}(A+C)\cos\theta_D$
$N(1650)$	$A_{1/2}$	$\frac{1}{6}(A+B-C)\sin\theta_S$
$\Delta(1620)$	$A_{1/2}$	$\frac{1}{18}(3A-B+C)$
$N(1700)$	$A_{1/2}$	$\frac{1}{6\sqrt{2}}(A-2B-C)\sin\theta_D$
	$A_{3/2}$	$\frac{1}{2\sqrt{6}}(A+C)\sin\theta_D$
$\Delta(1700)$	$A_{1/2}$	$\frac{1}{18\sqrt{2}}(3A+2B+C)$
	$A_{3/2}$	$\frac{1}{6\sqrt{6}}(3A-C)$

Table 1. Amplitudes $A_{1/2}$ and $A_{3/2}$ estimated by SQTM for the proton targets ($N = p$) [6, 7]. The angle θ_S is the mixing angle associated with the $N\frac{1}{2}^-$ states ($\theta_S = 31°$). The angle θ_D is the mixing angle associated with the $N\frac{3}{2}^-$ states ($\theta_S = 6°$).

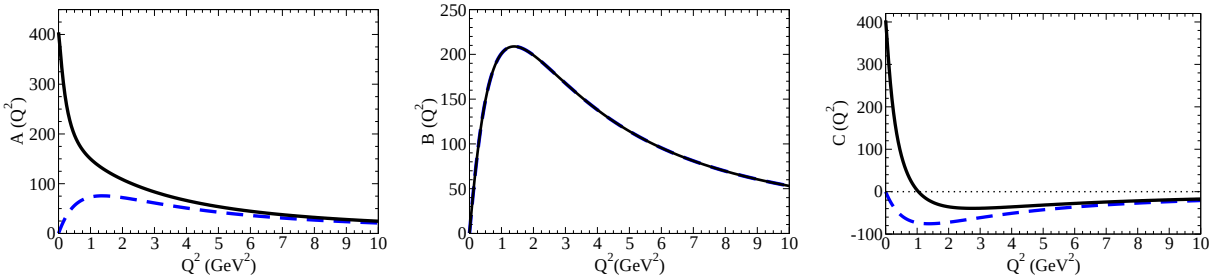

Figure 3. Results for the coefficients A, B and C for the model 1 (dashed-line) and model 2 (solid-line). In the model 1: $C = -A$.

In particular, the SQTM can be used to parametrize the $\gamma^* N \to N^*$ transitions, where N^* is a N (isospin 1/2) or a Δ (isospin 3/2) state from the $[70, 1^-]$ multiplet, in terms on three independent functions of Q^2: A, B, and C [6, 26]. The relations between the functions A, B, and C and the amplitudes are presented in the Table 1. Using the results for the $\gamma^* N \to N(1535)$ and $\gamma^* N \to N(1520)$ amplitudes, respectively $A^{S11}_{1/2}$, $A^{D13}_{1/2}$, and $A^{D13}_{3/2}$ in the spectroscopic notation, we can write

$$A = 2\frac{A^{S11}_{1/2}}{\cos\theta_S} + \sqrt{2}A^{D13}_{1/2} + \sqrt{6}A^{D13}_{3/2}, \qquad B = 2\frac{A^{S11}_{1/2}}{\cos\theta_S} - 2\sqrt{2}A^{D13}_{1/2},$$
$$C = -2\frac{A^{S11}_{1/2}}{\cos\theta_S} - \sqrt{2}A^{D13}_{1/2} + \sqrt{6}A^{D13}_{3/2}. \tag{7}$$

Once the coefficients A, B, and C, are determined, we can predict the amplitudes for the the transitions $\gamma^* N \to N(1650)$, $\gamma^* N \to N(1700)$, $\gamma^* N \to \Delta(1620)$ and $\gamma^* N \to \Delta(1700)$. Based on the amplitudes used in the calibration we expect the estimates to be accurate for $Q^2 \gtrsim 2$ GeV^2 [7].

From the relations (7) we can conclude in the limit where no meson cloud is considered ($A^{D13}_{3/2} = 0$) one has $C = -A$. That case defines the our model 1, and only the parameters A and B are necessary (since $C = -A$). When we have a (non-zero) parametrization for $A^{D13}_{3/2}$, we define the model 2. Using the parametrization discussed in the previous section we obtain the results for A, B and C presented in figure 3.

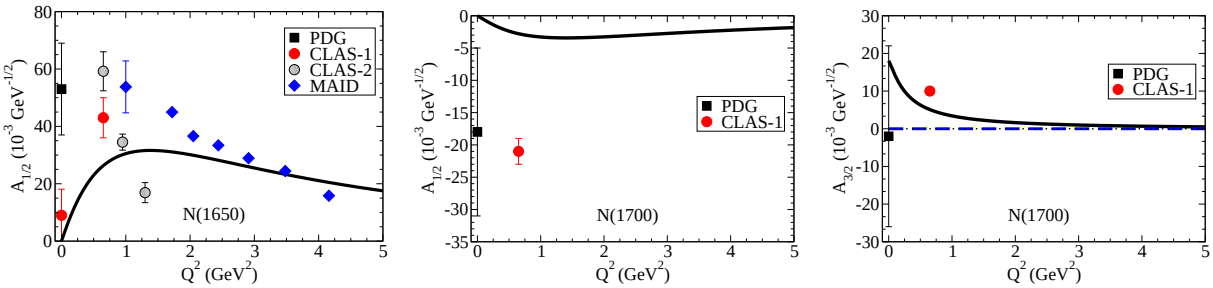

Figure 4. Results for the resonances $N(1650)$ and $N(1700)$. Model 1 (dashed-line) and Model 2 (solid-line). Data from [3, 27, 28, 29].

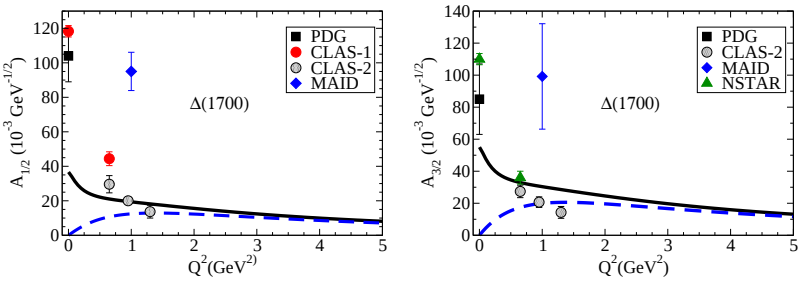

Figure 5. Results for the resonance $\Delta(1700)$. Model 1: dashed-line; Model 2: solid line. Data from [3, 27, 28, 29, 30].

5. Results

With the results of the functions A, B and C, represented in figure 3, for the model 1 (dashed-line) and model 2 (solid-line), it is possible to calculate the amplitudes for the remaining transition of the multiplet $[70, 1^-]$ using the relations from table 1.

The results are compared with data from CLAS (CLAS-1) [3, 27], preliminary data from CLAS (CLAS-2) [28], data from the MAID analysis [4], data presented in proceedings and workshops (NSTAR) [1, 6] and PDG data for $Q^2 = 0$ [29].

The results for the states $N(1650)$ and $N(1700)$ are on figure 4. In the graphs, we can see that the model 2 gives a better description for the amplitude $A_{3/2}$ (the model 1 gives $A_{3/2} \equiv 0$). Both models have the same result for $N(1650)$ which describe well the MAID data for $Q^2 \gtrsim 2$ GeV^2.

The results for the Δ states are presented in the figures 5 and 6, respectively for $\Delta(1700)$ and $\Delta(1650)$. For $\Delta(1700)$ we can see that the 2 models have very similar results for $Q^2 \gtrsim 1$ GeV^2. As for $\Delta(1650)$ only the model 2 has a good description of the data for $Q^2 \gtrsim 1$ GeV^2. The model 1 predicts negative values for the amplitude $A_{1/2}$.

We can conclude then, in general, that only the model 2 gives a good description of the data, particularly for $Q^2 \gtrsim 2$ GeV^2. Note that the model 2 is the model that takes into account the meson cloud effects ($A_{3/2}^{D13} \neq 0$).

Based on the expected behavior for large Q^2 given by $A_{1/2} \propto 1/Q^3$ and $A_{1/2} \propto 1/Q^5$ in accordance with perturbative QCD arguments [31], we parametrize the amplitudes as

$$A_{1/2}(Q^2) = D\left(\frac{\Lambda^2}{\Lambda^2 + Q^2}\right)^{3/2}, \qquad A_{3/2}(Q^2) = D\left(\frac{\Lambda^2}{\Lambda^2 + Q^2}\right)^{5/2}, \tag{8}$$

for $Q^2 \approx 5$ GeV^2. In the previous expression D and Λ are respectively coefficients and cutoffs dependent on the amplitude and on the resonance. The results of the parametrizations are in table 2. Those results may be useful to compare with future experiments at large Q^2 as the ones predicted for the Jlab-12 GeV upgrade [1].

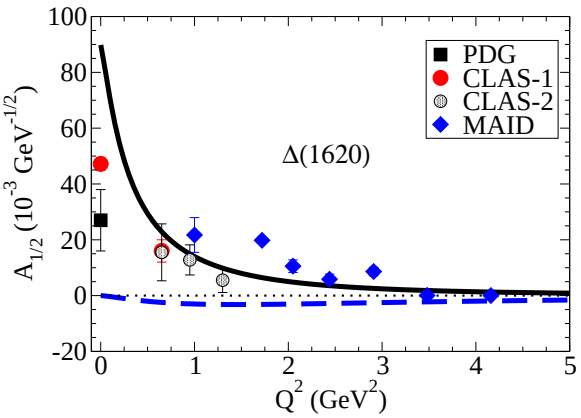

Figure 6. Results for $\Delta(1620)$. Note that only the model 2 (solid-line) has the correct sign.

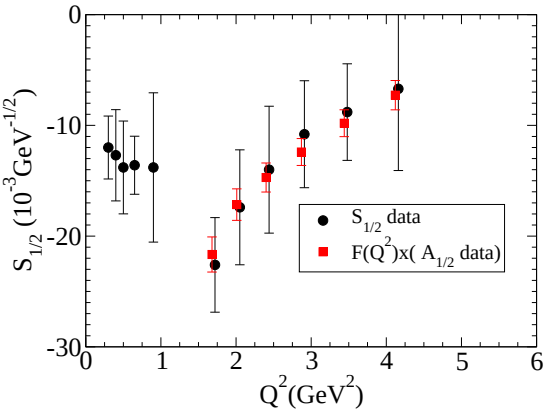

Figure 7. Relation between the amplitudes $A_{1/2}$ and $S_{1/2}$ for the $\gamma^*N \to N(1535)$ transition. $F(Q^2) = -\frac{\sqrt{1+\tau}}{\sqrt{2}}\frac{M_S^2-M^2}{2M_SQ}$.

State	Amplitude	$D(10^{-3}\mathrm{GeV}^{-1/2})$	$\Lambda^2(\mathrm{GeV}^2)$
$N(1650)$	$A_{1/2}$	68.90	3.35
$\Delta(1620)$	$A_{1/2}$	...	...
$N(1700)$	$A_{1/2}$	-8.51	2.82
	$A_{3/2}$	4.36	3.61
$\Delta(1700)$	$A_{1/2}$	39.22	2.69
	$A_{3/2}$	42.15	8.42

Table 2. Parameters from the high Q^2 parametrization given by equations (8).

For the amplitude $A_{1/2}$ associated with the $\Delta(1620)$ state it was not possible to find a parametrization consistent the power 3/2 as in equation (8). This happens because for that particular amplitude there is a partial cancellation between the leading terms (on $1/Q^3$) of our A, B and C parametrization due to the difference of sign between the amplitudes $A_{1/2}^{S11}$ and $A_{1/2}^{D13}$ used in the determination of the SQTM coefficients (see dashed-line on figure 6). As consequence the amplitude $A_{1/2}$ for the state $\Delta(1620)$ is dominated by next leading terms (on $1/Q^5$) or contributions due to meson cloud effects ($A_{3/2}^{D13}$). It is clear in figure 6 that, when we neglect the contributions from $A_{3/2}^{D13}$, the result correspondent to the model 1 (dashed-line) is almost zero. This result shows that in the $\gamma^*N \to \Delta(1620)$ transition, contrarily to what is usually expected, there is a strong suppression of the valence quark effects for $Q^2 = 1$–2 GeV^2. For a more detailed discussion see [7]. A simple parametrization of the amplitudes $A_{1/2}$ derived from our model is $A_{1/2} = 77.21\left(\frac{\Lambda^2}{\Lambda^2+Q^2}\right)^{5/2}$ in units 10^{-3} GeV$^{-1/2}$, with $\Lambda^2 = 1$ GeV^2. Note in particular the power 5/2, instead of the expected 3/2.

Another interesting prediction relatively to the helicity amplitudes of baryons with negative parity is the correlation between the amplitudes $A_{1/2}$ and $S_{1/2}$ associated with the $\gamma^*N \to N(1535)$ transition. The consequence of the experimental result, $F_2^* \approx 0$, observed for $Q^2 \gtrsim 1.5$ GeV^2 is that we can write in that regime $S_{1/2} = -\frac{\sqrt{1+\tau}}{\sqrt{2}}\frac{M_S^2-M^2}{2M_SQ}A_{1/2}$, where $\tau = \frac{Q^2}{(M_S+M)^2}$ [9]. The correlation between the 2 amplitudes is shown on figure 7.

6. Summary and conclusions

We combine the frameworks of the covariant spectator quark model and the single quark transition model in order to make predictions for the helicity amplitudes associated with negative parity resonances in the region of masses $W = 1.5$–1.8 GeV. The predictions are expected to be valid for $Q^2 \gtrsim 2$ GeV^2. Simple parametrizations for the amplitudes are calculated to facilitate the comparison with future experiments for $Q^2 \gtrsim 5$ GeV^2. Contrarily to what it was expected, in some transitions, like for the resonances $N(1535)$ and $\Delta(1620)$, the valence quark effects are not dominant in the region $Q^2 = 1$– 2 GeV^2.

Acknowledgments

The author thanks Kumar Gupta for comments and suggestions. The author was supported by the Brazilian Ministry of Science, Technology and Innovation (MCTI-Brazil).

References

[1] Aznauryan I G, Bashir A, Braun V, Brodsky S J, Burkert V D, Chang L, Chen C, El-Bennich B *et al.* 2013 *Int. J. Mod. Phys. E* **22**, 1330015.
[2] Aznauryan I G and Burkert V D 2012 *Prog. Part. Nucl. Phys.* **67**, 1.
[3] Aznauryan I G *et al.* [CLAS Collaboration] 2009 *Phys. Rev. C* **80**, 055203.
[4] Drechsel D, Kamalov S S, Tiator L 2007 *Eur. Phys. J. A* **34**, 69; Tiator T, Drechsel D, Kamalov S S, Vanderhaeghen M 2011 *Eur. Phys. J. ST* **198**, 141.
[5] Capstick S, Roberts W 2000 *Prog. Part. Nucl. Phys.* **45**, S241.
[6] Burkert V D, De Vita R, Battaglieri M, Ripani M and Mokeev V 2003 *Phys. Rev. C* **67**, 035204.
[7] Ramalho G 2014 *Phys. Rev. D* **90**, 033010.
[8] Gross F, Ramalho G and Peña M T 2008 *Phys. Rev. C* **77**, 015202.
[9] Ramalho G and Peña M T 2011 *Phys. Rev. D* **84**, 033007; Ramalho G and Tsushima K 2011 *Phys. Rev. D* **84**, 051301.
[10] Ramalho G and Peña M T 2014 *Phys. Rev. D* **89**, 094016.
[11] Gross F 1969 *Phys. Rev.* **186**, 1448; Stadler A, Gross F and Frank M 1997 *Phys. Rev. C* **56**, 2396.
[12] Gross F, Ramalho G and Peña M T 2012 *Phys. Rev. D* **85**, 093005.
[13] Ramalho G and Tsushima K 2011 *Phys. Rev. D* **84**, 054014; Ramalho G, Tsushima K and Thomas A W 2013 *J. Phys. G* **40**, 015102. Phys. Rev. D **84**, 054014 (2011);
[14] Ramalho G, Tsushima K and Gross F 2009 *Phys. Rev. D* **80**, 033004.
[15] Ramalho G and Peña M T 2009 *J. Phys. G* **36**, 115011.
[16] Ramalho G and Tsushima K 2013 *Phys. Rev. D* **87**, 093011; *Phys. Rev. D* **88**, 053002.
[17] Ramalho G and Tsushima K 2010 *Phys. Rev. D* **81**, 074020; Ramalho G and Tsushima K 2014 *Phys. Rev. D* **89**, 073010.
[18] Ramalho G and Peña M T 2009 *Phys. Rev. D* **80**, 013008.
[19] Ramalho G, Peña M T and Gross F 2008 *Eur. Phys. J. A* **36**, 329; *Phys. Rev. D* **78**, 114017; Ramalho G, Peña M T and Gross F 2010 *Phys. Rev. D* **81**, 113011; Ramalho G, Peña M T and Stadler A 2012 *Phys. Rev. D* **86**, 093022.
[20] Ramalho G and Tsushima K 2010 *Phys. Rev. D* **82**, 073007.
[21] Ramalho G and Tsushima K 2012 *Phys. Rev. D* **86**, 114030; Ramalho G and Peña M T 2011 *Phys. Rev. D* **83**, 054011; Ramalho G, Jido D and Tsushima K 2012 *Phys. Rev. D* **85**, 093014.
[22] Ramalho G and Peña M T 2012 *Phys. Rev. D* **85**, 113014.
[23] Gross F, Ramalho G, Peña M T 2012 *Phys. Rev. D* **85**, 093006.
[24] Ramalho G and Tsushima K, to be submitted.
[25] Sato T, Lee T-S L 2009 *J. Phys. G* **36**, 073001.
[26] Hey A J G and Weyers 1974 *Phys. Lett. B* **48**, 69; Cottingham W N and Dunbar I H 1979 *Z. Phys. C* **2**, 41.
[27] Dugger M *et al.* [CLAS Collaboration] 2009 *Phys. Rev. C* **79**, 065206.
[28] Mokeev V I *et al.* [CLAS Collaboration] 2012 *Phys. Rev. C* **86**, 035203.
[29] Beringer J *et al.* [Particle Data Group Collaboration] 2012 *Phys. Rev. D* **86**, 010001.
[30] Electromagnetic N-N* Transition Form Factors Workshop, Jlab, Newport News, 2008 (unpublished)
[31] Carlson C E and Poor J L 1998 *Phys. Rev. D* **38**, 2758.